Relativistic Hartree-Bogoliubov description of sizes and shapes of A=20 isobars

Lalazissis, G. A.; Vretenar, Dario; Ring, Peter

Source / Izvornik: **Physical Review C - Nuclear Physics, 2001, 63, 34305 - 5**

Journal article, Published version
Rad u časopisu, Objavljena verzija rada (izdavačev PDF)

https://doi.org/10.1103/PhysRevC.63.034305

Permanent link / Trajna poveznica: https://urn.nsk.hr/urn:nbn:hr:217:533631

Relativistic Hartree-Bogoliubov description of sizes and shapes of $A=20$ isobars

G. A. Lalazissis,[1,2] D. Vretenar,[1,3] and P. Ring[1]
[1]*Physik-Department der Technischen Universität München, D-85748 Garching, Germany*
[2]*Physics Department, Aristotle University of Thessaloniki, Thessaloniki GR-54006, Greece*
[3]*Physics Department, Faculty of Science, University of Zagreb, 10 000 Zagreb, Croatia*
(Received 25 September 2000; published 9 February 2001)

Ground-state properties of $A=20$ nuclei (^{20}N, ^{20}O, ^{20}F, ^{20}Ne, ^{20}Na, and ^{20}Mg) are described in the framework of relativistic Hartree-Bogoliubov theory. The model uses the $NL3$ effective interaction in the mean-field Lagrangian, and describes pairing correlations by the pairing part of the finite-range Gogny interaction $D1S$. Binding energies, quadrupole deformations, nuclear matter radii, and differences in radii of proton and neutron distributions are compared with recent experimental data.

DOI: 10.1103/PhysRevC.63.034305 PACS number(s): 21.60.Jz, 21.10.Dr, 21.10.Gv, 27.30.+t

I. INTRODUCTION

Sizes, shapes, and binding energies are fundamental characteristics of nuclei and reflect the basic properties of effective nuclear forces. The description of the generalized moments of the nuclear density distributions provides an important test for nuclear structure models. In particular, a description of ground-state properties of an isobaric sequence of nuclei tests the isovector channel of the effective nuclear force. The correct parametrization of this channel is essential for the description of structure phenomena in exotic nuclei far from β stability. In the present study we analyze the sequence of $A=20$ nuclei: ^{20}N, ^{20}O, ^{20}F, ^{20}Ne, ^{20}Na, and ^{20}Mg. Experimental data on nuclear-matter radii derived from the measured interaction cross section of these nuclei have been reported in Ref. [1]. Evidence has been found for the existence of a proton skin for ^{20}Mg and of a neutron skin for ^{20}N. The largest difference in radii (≈ 0.2 fm) has been reported for the mirror nuclei ^{20}O and ^{20}Mg. This last result has prompted several theoretical investigations, but the extremely small value for the matter radius of ^{20}O has not been reproduced in calculations that include the microscopic three-cluster model [2], the Hartree-Fock model with Skyrme interactions [3–6], a single-particle potential model [5], and the shell-model [6]. The experimental data on interaction cross sections of $A=20$ isobars were also reviewed in Ref. [7] by using a variety of phenomenological and semimicroscopic models.

In the present analysis of the $A=20$ isobaric sequence we employ the relativistic Hartree-Bogoliubov (RHB) theory. Based on the relativistic mean-field theory and on the Hartree-Fock-Bogoliubov framework, the RHB theory provides a unified description of mean-field and pairing correlations. It has been successfully applied to the description of nuclear structure phenomena, not only in nuclei along the valley of β stability, but also of exotic nuclei close to the particle drip lines. In particular, applications relevant to the present study include: the halo phenomenon in light nuclei [8], properties of light nuclei near the neutron drip [9], reduction of the spin-orbit potential in nuclei with extreme isospin values [10], the deformation and shape coexistence phenomena that result from the suppression of the spherical $N=28$ shell gap in neutron-rich nuclei [11], properties of proton-rich nuclei, and the phenomenon of ground-state proton radioactivity [12,13].

The relativistic mean-field theory is based on simple concepts [14]: nucleons are described as point particles, the theory is fully Lorentz invariant, the nucleons move independently in mean fields that originate from the nucleon-nucleon interaction. Conditions of causality and Lorentz invariance impose that the interaction is mediated by the exchange of pointlike effective mesons, which couple to the nucleons at local vertices. The single-nucleon dynamics is described by the Dirac equation

$$\left\{-i\boldsymbol{\alpha}\cdot\boldsymbol{\nabla}+\beta(m+g_\sigma\sigma)+g_\omega\omega^0+g_\rho\tau_3\rho_3^0+e\frac{(1-\tau_3)}{2}A^0\right\}\psi_i = \varepsilon_i\psi_i, \tag{1}$$

where σ, ω, and ρ are the meson fields, A denotes the electromagnetic potential, and g_σ, g_ω, and g_ρ are the corresponding coupling constants for the mesons to the nucleon. The lowest order of the quantum-field theory is the *mean-field* approximation: the meson-field operators are replaced by their expectation values. The sources of the meson fields are defined by the nucleon densities and currents. The ground state of a nucleus is described by the stationary self-consistent solution of the coupled system of Dirac and Klein-Gordon equations.

In addition to the self-consistent mean-field potential, pairing correlations have to be included in order to describe ground-state properties of open-shell nuclei. In the framework of the relativistic Hartree-Bogoliubov model, the ground state of a nucleus $|\Phi\rangle$ is represented by the product of independent single-quasiparticle states. These states are eigenvectors of the generalized single-nucleon Hamiltonian that contains two average potentials: the self-consistent mean-field $\hat{\Gamma}$ that encloses all the long-range particle-hole (ph) correlations, and a pairing field $\hat{\Delta}$ that sums up the particle-particle (pp) correlations. In the Hartree approximation for the self-consistent mean field, the relativistic Hartree-Bogoliubov equations read

$$\begin{pmatrix} \hat{h}_D - m - \lambda & \hat{\Delta} \\ -\hat{\Delta}^* & -\hat{h}_D + m + \lambda \end{pmatrix} \begin{pmatrix} U_k(\mathbf{r}) \\ V_k(\mathbf{r}) \end{pmatrix} = E_k \begin{pmatrix} U_k(\mathbf{r}) \\ V_k(\mathbf{r}) \end{pmatrix}, \tag{2}$$

where $\hat{h}_D$ is the single-nucleon Dirac Hamiltonian (1), and m is the nucleon mass. The chemical potential λ has to be determined by the particle number subsidiary condition in order that the expectation value of the particle number operator in the ground state equals the number of nucleons. $\hat{\Delta}$ is the pairing field. The column vectors denote the quasiparticle spinors and E_k are the quasiparticle energies. The RHB equations are solved self-consistently, with potentials determined in the mean-field approximation from solutions of Klein-Gordon equations for the sigma meson, omega meson, rho meson, and photon field, respectively.

II. GROUND-STATE PROPERTIES OF $A=20$ ISOBARS

The details of the ground-state properties of the $A=20$ isobaric sequence will depend on the choice of the effective nuclear interaction. In the last few years several new and more accurate parameter sets of meson masses and meson-nucleon coupling constants for the effective mean-field Lagrangian have been derived. Due to large uncertainties in the experimental data, older effective interactions were not specifically designed to describe ground-state isovector properties. Only more recently have isovector properties been included in the set of data on which the effective interactions are adjusted. In the relativistic mean-field model, perhaps the most accurate set of meson masses and meson-nucleon coupling constants is $NL3$ [15]. In most recent applications of the RHB theory we have used the $NL3$ effective interaction for the mean-field Lagrangian, and the pairing field has been described by the pairing part of the Gogny interaction with the $D1S$ parameter set [16]. This force has been very carefully adjusted to the pairing properties of finite nuclei all over the periodic table. In particular, the basic advantage of the Gogny force is the finite range, which automatically guarantees a proper cutoff in momentum space.

The RHB equations are solved self-consistently, with potentials determined in the mean-field approximation from solutions of Klein-Gordon equations for the meson fields. The Dirac-Hartree-Bogoliubov equations and the equations for the meson fields are solved by expanding the nucleon spinors $U_k(\mathbf{r})$ and $V_k(\mathbf{r})$, and the meson fields in terms of the eigenfunctions of a deformed axially symmetric oscillator potential. The calculations for the present analysis have been performed by an expansion in 12 oscillator shells for the fermion fields, and 20 shells for the boson fields. We have verified that identical results for the binding energies, rms radii, and ground-state deformation parameters are obtained by expanding the fermion fields in 14 and 16 oscillator shells. A simple blocking procedure is used in the calculation of odd-proton and/or odd-neutron systems. The blocking calculations are performed without breaking the time-reversal symmetry. A detailed description of the relativistic Hartree-Bogoliubov model for deformed nuclei can be found in Ref. [13].

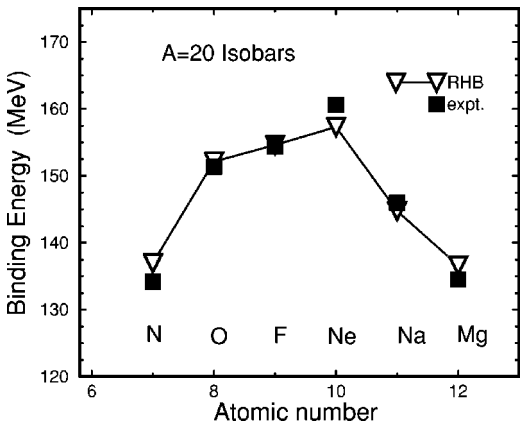

FIG. 1. Binding energies of $A=20$ nuclei calculated with the $NL3$ + Gogny $D1S$ effective interaction. The theoretical values are compared with the experimental binding energies [17].

In Fig. 1 we compare the RHB $NL3+D1S$ binding energies of the $A=20$ nuclei (^{20}N, ^{20}O, ^{20}F, ^{20}Ne, ^{20}Na, and ^{20}Mg) with experimental data [17]. The agreement between theory and experiment is very good. The self-consistent RHB neutron and proton ground-state density distributions for the $A=20$ isobaric sequence are shown in Fig. 2. We will eventually compare the calculated radii with experimental values, but here we notice the trend: a pronounced proton skin is observed in ^{20}Mg, it slowly disappears and the proton and neutron density distributions are almost identical in ^{20}Ne, the neutron skin develops and is very pronounced in ^{20}N. This trend is in complete agreement with experimental evidence for the existence of a proton skin for ^{20}Mg and of a neutron skin for ^{20}N [1].

The calculated ground-state quadrupole deformations of $A=20$ isobars are shown in Fig. 3 as function of the isospin projection T_z. Except for ^{20}Ne and ^{20}Na, the $A=20$ nuclei

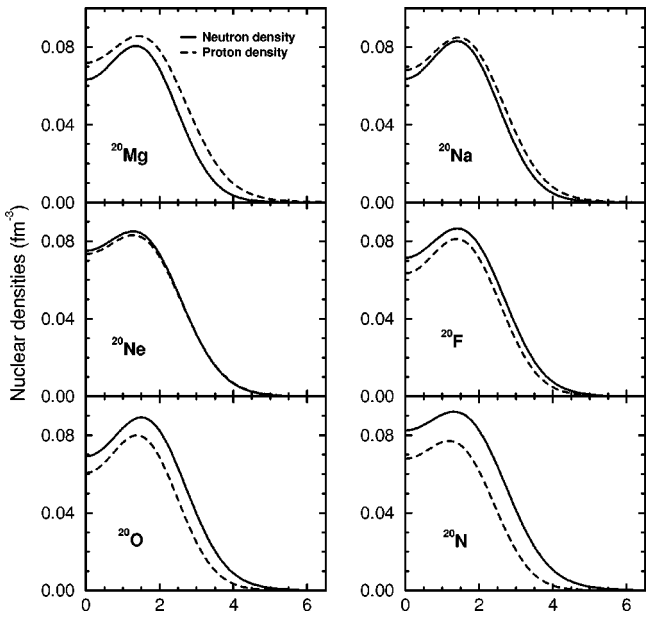

FIG. 2. Self-consistent RHB neutron and proton ground-state density distributions of $A=20$ nuclei.

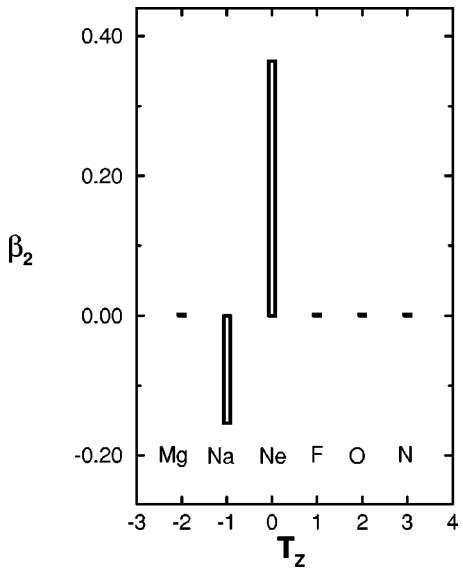

FIG. 3. Calculated ground-state quadrupole deformations of $A=20$ isobars as a function of the isospin projection T_z.

are essentially spherical. ^{20}Ne is strongly prolate deformed ($\beta_2=0.365$), and an oblate ground state is calculated for ^{20}Na ($\beta_2=-0.153$). The surface thickness and diffuseness parameters of the proton and neutron density distributions (Fig. 1) are displayed in Fig. 4. The surface thickness s is defined to be the change in radius required to reduce $\rho(r)/\rho_0$ from 0.9 to 0.1 (ρ_0 is the density in the center of the nucleus). The diffuseness parameter α is determined by fitting the neutron density profiles to the Fermi distribution

$$\rho(r)=\rho_0\left[1+\exp\left(\frac{r-R_0}{\alpha}\right)\right]^{-1}, \tag{3}$$

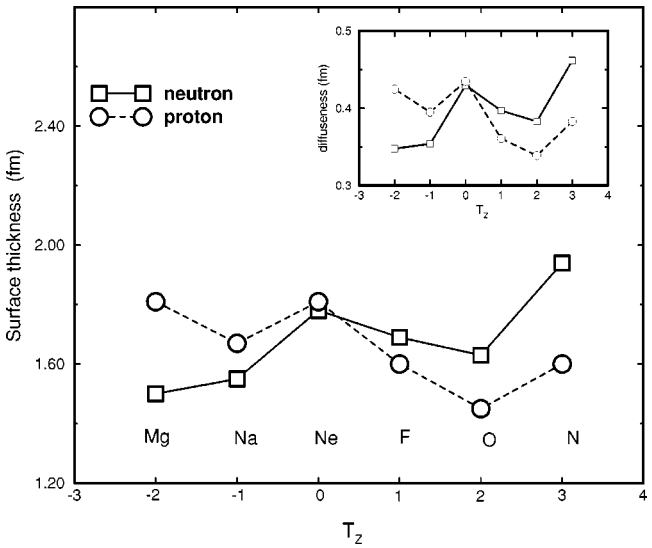

FIG. 4. Surface thickness of the neutron and proton density distributions of the $A=20$ isobars, calculated with the $NL3+$ Gogny $D1S$ effective interaction. In the insert the corresponding values for diffuseness parameter are included.

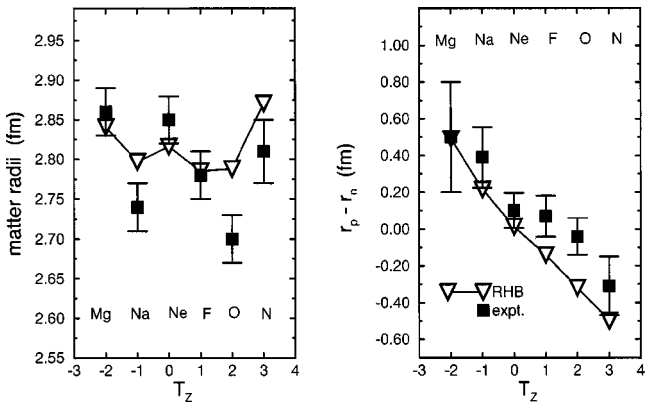

FIG. 5. The nuclear-matter radii (left), and the differences between proton and neutron radii (right) of the $A=20$ nuclei as functions of the isospin projection T_z. Results of fully self-consistent RHB calculations are compared with experimental data [1].

where R_0 is the half-density radius. The surface thickness and diffuseness parameters quantify the proton and neutron skins: for ^{20}Mg $s(p)=1.81$ fm, $s(n)=1.50$ fm, and the corresponding diffuseness parameters $\alpha(p)=0.42$ fm, $\alpha(n)=0.35$ fm; for ^{20}N $s(p)=1.60$ fm, $s(n)=1.94$ fm, $\alpha(p)=0.38$ fm, $\alpha(n)=0.46$ fm. For ^{20}Ne the surface thickness and diffuseness parameters of the proton and neutron distributions are identical.

The calculated radii are compared with experimental data [1,18] in Figs. 5 and 6. In Fig. 5 we display the nuclear matter radii (left panel), and the differences between proton and neutron radii (right panel) of the $A=20$ nuclei as functions of the isospin projection T_z. The theoretical values are in good agreement with experimental data. The calculated matter radii reproduce the observed staggering between even and odd values of T_z. Somewhat larger discrepancies are, however, found for ^{20}Na and ^{20}O. Since the calculated proton radii for these two nuclei reproduce the experimental values (6), it appears that the RHB model calculations overestimate the neutron radii. We have verified that the calculated radii do not depend on our choice of the pairing inter-

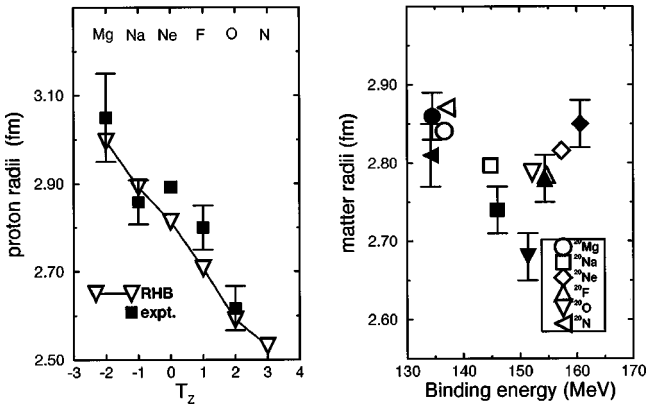

FIG. 6. Theoretical values for the proton radii as a function of the isospin projection T_z (left), and for the matter radii as a function of the binding energy (right) of the $A=20$ isobaric sequence, in comparison with experimental data [1].

action. In fact, even without pairing we calculate essentialy the same values for the rms radii. The reason is that, for nuclei that are not really close to the drip line, in a self-consistent RHB calculation the mean field partly compensates the omission of pairing correlations. For example, the calculated rms radius of the neutron distribution in ^{20}O is 2.925 fm, the pairing energy is 9.1 MeV, and the total binding energy is 154.4 MeV. If the pairing interaction is not included in the calculation, the resulting neutron rms radius is 2.923 fm and the total binding energy is 150.3 MeV. The differences between the calculated and experimental matter radii could perhaps be attributed to our choice of the $NL3$ effective interaction, which favors somewhat larger neutron radii, although this seems not to be the case for ^{20}Mg, ^{20}Ne, and ^{20}F. It is also possible that, for these relatively light nuclei, in some cases particle number projection (not performed in the present analysis) has a pronounced effect on the calculated ground-state properties.

For ^{20}O the calculated matter radius is 2.79 fm, while the experimental value is 2.69 (3) [1]. However, as we have already mentioned in the introduction, several theoretical models have failed to reproduce this extremely small value for the matter radius of ^{20}O [3,4,2,5], and it was also suggested that the reported experimental value should be reconsidered [5]. All theoretical calculations predict the matter radius in the interval between 2.77 fm and 2.83 fm, in agreement with the result of the present analysis. In fact, since most models predict overbinding for the O isotopes (^{26}O, and even ^{28}O, are bound nuclei in most model calculations), one would expect the theoretical value for the matter radius in ^{20}O to be smaller than the experimental one. We have also calculated the relative contributions of the valence orbitals to the rms radius of the neutron distribution. Without the inclusion of the pairing correlations, the four valence neutrons are in the $1d_{5/2}$ orbital, and they contribute 47% to the neutron rms radius. With the inclusion of the pairing interaction, also the $2s_{1/2}$ and the $1d_{3/2}$ orbitals become fractionally occupied. Their contribution to the neutron radius is, however, relatively small: 2.7% for the $2s_{1/2}$, and 2% for $1d_{3/2}$ orbital. 41.5% is the relative contribution of the $1d_{5/2}$ orbital. As discussed above, the total neutron radius is practically unaffected by the inclusion of pairing correlations.

With the exception of ^{20}O, also the calculated differences between proton and neutron radii (right panel) are in good agreement with experimental data. In particular, the theoretical values agree with the large differences found in nuclei with a large excess of neutrons (^{20}N, 0.33 ± 0.15 fm) or protons (^{20}Mg, 0.50 ± 0.28 fm).

Finally, in Fig. 6 theoretical and experimental values are compared for the proton radii as function of the isospin projection T_z (left panel), and for the matter radii as function of the binding energy. We notice a very good agreement for all the proton radii. The RHB model also reproduces, with the above-discussed exception of ^{20}O, the functional dependence of the matter radii on the binding energy of the $A = 20$ nuclei.

III. SUMMARY

In this study we have applied the relativistic Hartree-Bogoliubov theory in an analysis of ground-state properties of nuclei that belong to the $A=20$ isobaric sequence. The $NL3$ effective interaction has been used for the mean-field Lagrangian, and pairing correlations have been described by the pairing part of the finite-range Gogny interaction $D1S$. This particular combination of effective forces in the ph and pp channels has been used in most of our recent applications of the RHB theory. Theoretical predictions for binding energies, neutron and proton ground-state density distributions, quadrupole deformations, nuclear matter radii, proton radii, and differences between proton and neutron radii for ^{20}N, ^{20}O, ^{20}F, ^{20}Ne, ^{20}Na, and ^{20}Mg have been analyzed and compared with available experimental data. It has been shown that the $NL3$ effective force provides a very good description of the observed ground-state properties as function of the isospin projection T_z. The results of the present analysis confirm that the isovector channel of the $NL3$ interaction is correctly parametrized and that this effective force can be used to describe properties of nuclei far from β stability.

ACKNOWLEDGMENTS

This work has been supported in part by the Bundesministerium für Bildung und Forschung under Project No. 06 TM 979, by the Deutsche Forschungsgemeinschaft, and by the Gesellschaft für Schwerionenforschung (GSI), Darmstadt.

[1] L. Chulkov *et al.*, Nucl. Phys. **A603**, 219 (1996).
[2] P. Descouvemont, Phys. Lett. B **437**, 7 (1998).
[3] B.A. Brown and P.G. Hansen, Phys. Lett. B **381**, 391 (1996).
[4] H. Kitagawa, N. Tajima, and H. Sagawa, Z. Phys. A **358**, 381 (1997).
[5] R. Sherr, H.T. Fortune, and B.A. Brown, Eur. Phys. J. A **5**, 371 (1999).
[6] T. Siiskonen, P.O. Lipas, and J. Rikovska, Phys. Rev. C **60**, 034312 (1999).
[7] O.M. Knyaz'kov, I.N. Kukhtina, and S.A. Fayans, Fiz. Elem. Chastits At. Yadra **30**, 870 (1999) [Phys. Part. Nucl. **30**, 369 (1999)].
[8] W. Pöschl, D. Vretenar, G.A. Lalazissis, and P. Ring, Phys. Rev. Lett. **79**, 3841 (1997).
[9] G.A. Lalazissis, D. Vretenar, W. Pöschl, and P. Ring, Nucl. Phys. **A632**, 363 (1998).
[10] G.A. Lalazissis, D. Vretenar, W. Pöschl, and P. Ring, Phys. Lett. B **418**, 7 (1998).
[11] G.A. Lalazissis, D. Vretenar, P. Ring, M. Stoitsov, and L. Robledo, Phys. Rev. C **60**, 014310 (1999).
[12] D. Vretenar, G.A. Lalazissis, and P. Ring, Phys. Rev. Lett. **82**, 4595 (1997).

[13] G.A. Lalazissis, D. Vretenar, and P. Ring, Nucl. Phys. **A650**, 133 (1999).
[14] P. Ring, Prog. Part. Nucl. Phys. **37**, 193 (1996).
[15] G.A. Lalazissis, J. König, and P. Ring, Phys. Rev. C **55**, 540 (1997).
[16] J.F. Berger, M. Girod, and D. Gogny, Nucl. Phys. **A428**, 32 (1984).
[17] G. Audi and A.H. Wapstra, Nucl. Phys. **A595**, 409 (1995).
[18] T. Suzuki *et al.*, Nucl. Phys. **A616**, 286c (1997).